

STRV CRYOCOOLER TIP MOTION SUPPRESSION

R. Glaser, R.G. Ross, Jr. and D.L. Johnson

Applied Mechanics Technologies Section
Jet Propulsion Laboratory
California Institute of Technology
Pasadena, California 91109

ABSTRACT

The Space Technology Research Vehicle (STRV-1b) scheduled to fly at the beginning of June 1994, has a cryocooler vibration suppression experiment aboard doing motion suppression of the tip of the coldfinger. STRV-1b is a bread box sized satellite to be launched on the next flight of the Ariane-4. To meet stringent power, weight, and space constraints, the experiment uses a tiny 1/5-watt 80K Texas Instruments tactical Stirling cooler. Two different tip-motion cancellation techniques are implemented in the experiment: 1) an applique ceramic stretching the coldfinger; and 2) three commercial low voltage piezo-electric translators that move the cryocooler supports. Motion of the coldfinger tip is measured in three dimensions to 10 nanometers using commercial eddy current transducers. Two different control systems are used: 1) an analog control system using a bandpass filter to suppress the cooler drive fundamental, and 2) a feed forward steady-state harmonic analyzer that continuously updates a command signal to each actuator.

INTRODUCTION

STRV-1a and 1b are small companion satellites flying with a communications satellite. All three satellites are awaiting a June resumption of Ariane-4 launches following a launch failure. The two STRV satellites are small rectangular satellites (480×480×400 mm) that will be left in the geostationary transfer orbit when the communications satellite is boosted to geostationary orbit. The STRV-1a and 1b are free flying, spin stabilized, solar powered satellites. Because of the small satellite size the STRV experiments are severely limited by power, thermal control, weight, and space.

The cryocooler experiment is shown in Fig. 1. The experiment is a technology demonstration to show piezo-electric vibration suppression technology is mature enough for space applications. A Texas Instruments 1/5 watt tactical Stirling cooler is used as a test bed. The objective of the experiment is to keep the tip of the coldfinger from moving. Two actuation techniques are employed: 1) piezo-electric translators move the entire cooler, and 2) ceramic appliques, glued to the base of the coldfinger, stretch the coldfinger itself. Coldfinger tip motion is measured by eddy current transducers. The eddy current transducers are mounted on a stiff ring inside the cooler that also supports the non-moving side of the translators. All three eddy current transducers are at the same angle to the coldfinger and at 90° to each other. Two types of

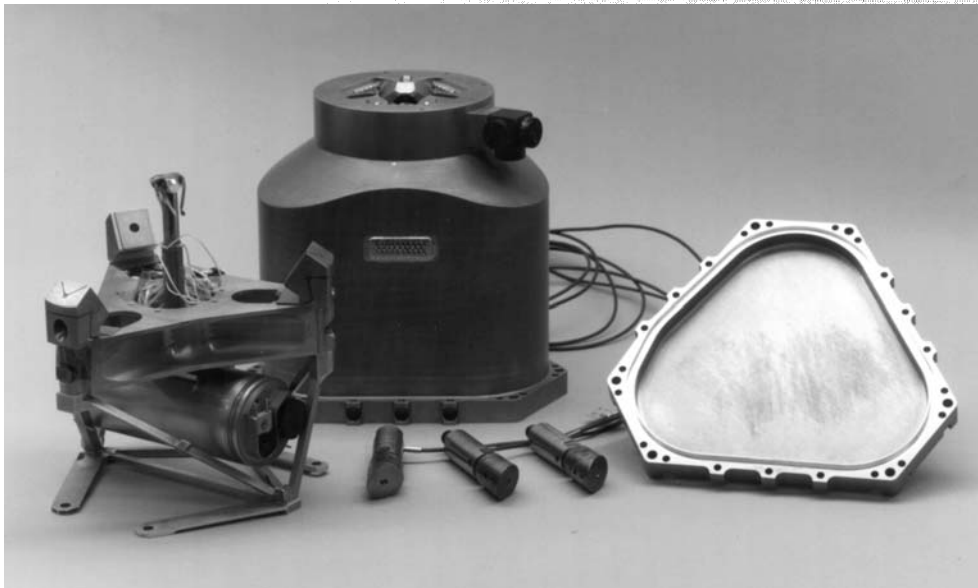


Figure 1. Cryocooler Experiment Configuration

control systems are used: 1) a bandpass analog control system that suppresses the first harmonic, and 2) a feed-forward harmonic based digital control system.

PIEZO-ELECTRIC TRANSLATORS

The piezo-electric translators are commercially available in a wide variety of sizes. The ones used on STRV-1b are piezo stacks where a series of very thin wafers have been electrically connected in parallel and mechanically connected in series. In previous generations of piezos, the wafers/electrodes were often bonded together with adhesives; the stacks flown on STRV-1b are made with a more sophisticated process and are solid blocks of material. The new-technology piezo stacks have the added advantage that they operate at a much lower voltage than the old stacks. This is because the wafer thickness is much smaller. The piezo-electric effect responds to the electrical field strength. Thinner wafers create the same field strength at the lower voltages. The actuators used on STRV-1b can operate between 0 and 100 volts. However, on STRV-1b only 20 volts were required.

The piezo stacks used on STRV-1b are contained in a cylindrical steel shell that protects the stack and provides a load path for the preload. To launch a ceramic, the material should always be under compression to avoid cracking. The preload system used in the STRV-1b actuators is a Belleville washer. The manufacturer normally doesn't preload the system to a high enough level that the actuator can take equal loads in compression and tension. It was necessary to sacrifice some stroke to provide the capability of surviving equal tension and compression loads during launch.

The actuators are sensitive to over-excitation. The initial set of three actuators used on STRV was accidentally destroyed (electrical insulation was broken down) when wideband white noise at over 100 volts was inadvertently applied. The failure caused electrical breakdown (shorting) when any significant voltage was applied to the stack. At very low voltages, the electrical properties of the stack were normal, but at any meaningful voltage the stack didn't operate.

Another problem encountered with the translators had to do with grounding. Normally electrical ground and mechanical ground are kept separated in a spacecraft. Unfortunately the actuator's case is electrical ground. This probably could be rectified by the manufacturer if requested.

APPLIQUE CERAMIC ACTUATORS

Unlike the translators, the applique ceramics are not a commercial product. The materials can be purchased in a variety of shapes, but using the materials is quite involved. For STRV-1b the objective was to glue three segments of a cylindrical ceramic to the coldfinger of the cooler. This is illustrated in Fig. 2.

Numerous issues arose:

- 1) the choice of glues.
- 2) maintaining electrical isolation from the coldfinger.
- 3) loss of piezo-electric effect due to the temperature of the coldfinger.
- 4) how to solder electrical connections to the delicate metal coating.
- 5) how to cut the ceramic tubes into three segments.
- 6) making electrical connections to the inside surface of the applique.
- 7) maintaining quality control on the glue line thickness.
- 8) how to apply preloads to the ceramics so they will not crack.
- 9) installing the moving regenerator element into the coldfinger tube, which becomes deformed by the piezo preload.

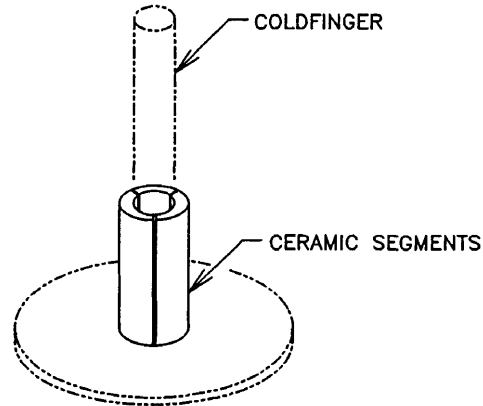


Figure 2. Ceramic Applique Actuators

These and other issues are discussed in detail in Reference 1.

Performance testing the cooler with an applique ceramic proved difficult. The ceramic is an excellent insulator so the heat loss through the ceramic applique was acceptably small. Unfortunately the heat capacity of the ceramic was significant enough that it was impossible to bring the system to equilibrium in a reasonable time. After eight hours of trying to reach an equilibrium temperature, the effort was abandoned. The STRV-1b is too power starved to operate at equilibrium. Most of the thermal testing was done under transient conditions.

ANALOG CONTROL SYSTEM

Originally the objective was to design a wideband analog controller covering the region below the support resonant frequencies. This approach had to be dropped when it was discovered that the stability margins would be inadequate. The control designer estimated there was approximately 10 Hz of stable bandwidth. The analog controller was switched to a bandpass controller working on the fundamental frequency. A bandpass controller was designed and one channel checked out early in the program. It was put aside while the hardware was built. Then the controller parameters (resistors and capacitors) were matched to the actual plant. The controller tracks frequency changes in the cooler because switched capacitor filters are used in the bandpass filter. The frequency source for the switched capacitor filters is programmable.

In addition to the controller it was necessary to build an analog circuit that caused motion at one eddy current transducer at a time. To do this, all three actuators have to be activated in a fixed ratio. The ratio was found by activating one actuator at a time and assembling the measured eddy current data into a three-by-three matrix. Then the matrix was numerically inverted and the circuit was set up to form the signals required.

The measured open loop transfer function for one channel of the analog controller is shown in the top figure of Fig. 3. The circuit diagram in Fig. 4 illustrates the wiring for this transfer function. When the controller is operating, the dotted lines in the circuit diagram are connected to the bandpass filters. To take the transfer function, the eddy current signals are disconnected

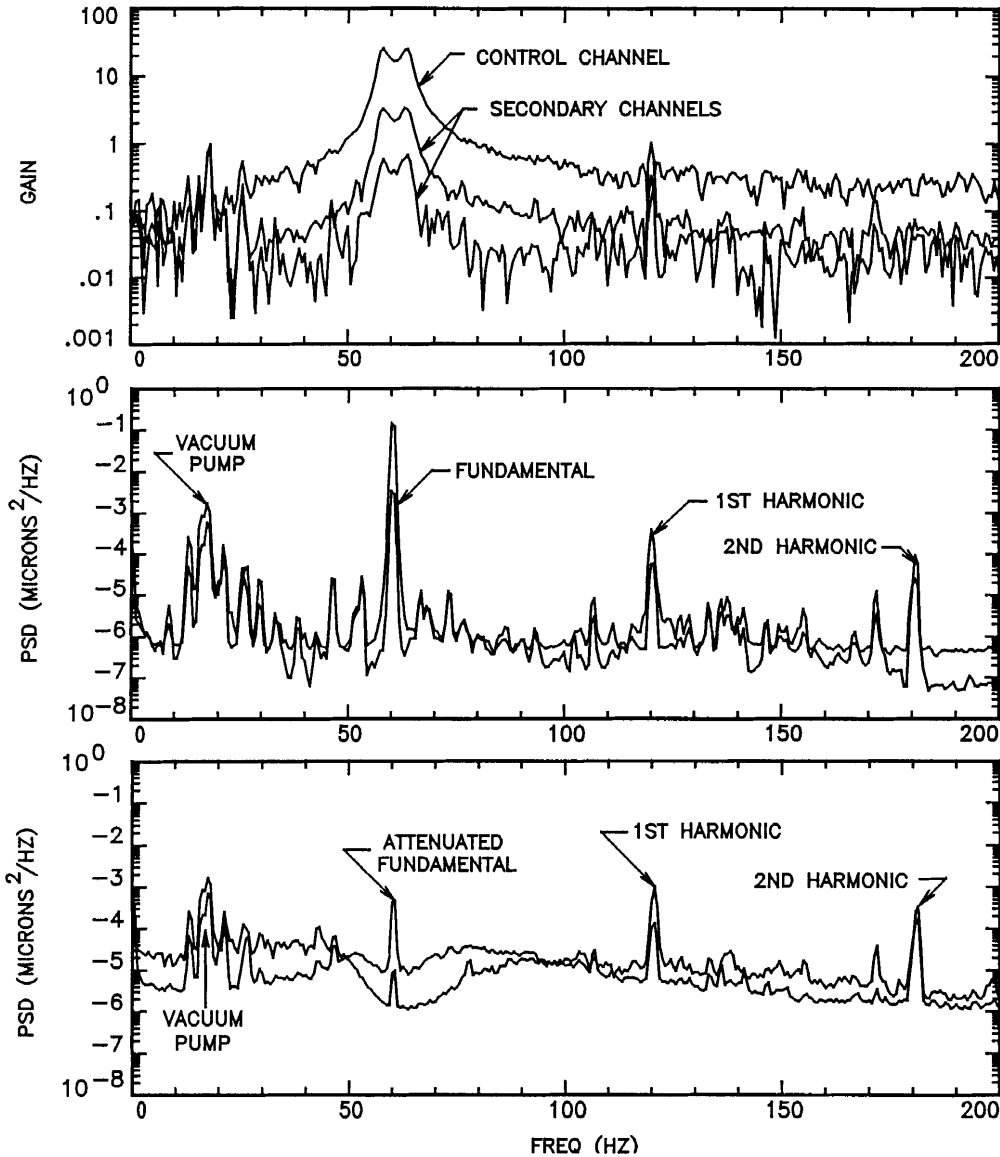


Figure 3. Analog Controller Frequency Domain Performance

and connected to the spectral analyzer instead. The random signal output of the spectral analyzer is run into one of the bandpass filters (the dashed line) and the three transfer functions shown in Fig. 3 are obtained.

The pass band can be seen as the area of the "control channel" curve above unity gain. In this area there is significant feedback canceling any disturbance. At frequencies away from the pass band the gain is much less than unity and the control system doesn't materially change the plant. Each bandpass filter channel is designed to suppress the motion of one of the three eddy current signals. In the example, all three ceramic applique segments are activated such that the coldfinger tip moves directly towards the number 1 eddy current transducer. The circuitry that does this in the block labelled "3x3 board." The other two signals in Fig. 3 are the measured outputs from the other two eddy current channels. If the 3x3 circuits were perfect, both channels would read a level at the noise floor, however, this level of accuracy is not really required.

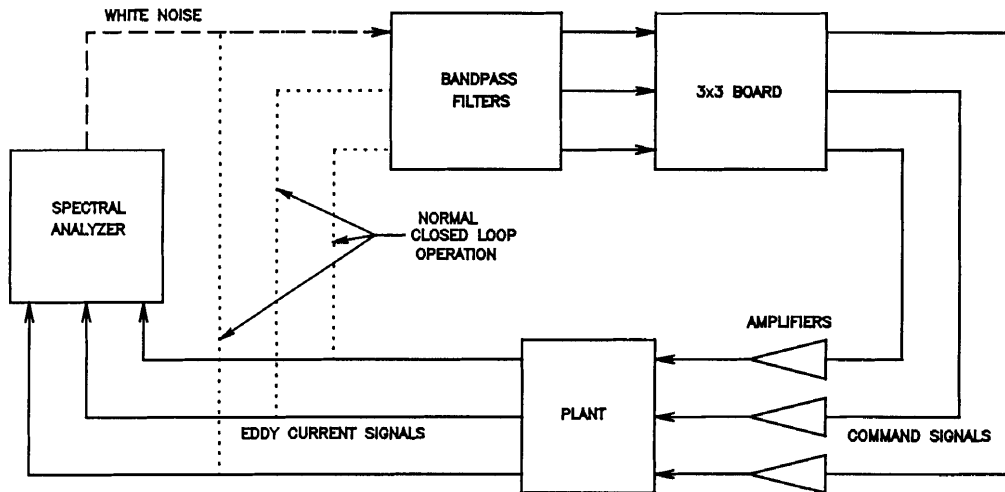


Figure 4. Analog Controller Circuit Diagram

The bottom two graphs in Fig. 3 show the closed loop results. The middle graph is a power spectral density (PSD) for all three eddy current transducers with the controller off. Turning the controller on, the same PSD results are shown in the lower graph. The controller reduces the fundamental by a factor of 400 in PSD, or approximately a factor of 20 in response. The transfer functions for the other two filters are very similar to the one illustrated.

This result is more dramatic in the time domain, as shown in Fig. 5. The time histories for the largest two channels are shown (channel 1 and channel 3). In the top figure there is a great deal of the fundamental frequency in the two signals. This data was taken with the control system off. Channel 3, in particular, is dominated by the fundamental frequency. The bottom figure illustrates the results with the control system turned on. The content of the fundamental frequency for both channels has been dramatically reduced. Of course, the other frequencies are still there, since the controller doesn't address them.

Both actuator power-supplies proved difficult. Piezo-electric actuators behave electrically like capacitors. Worse, they exhibit back EMF. The piezo-electric phenomenon is reversible. Voltage applied to the actuator creates motions, but also if the actuator is squeezed it creates voltages. When the actuator works against a spring such as the preload, the piezo-electric material releases stored strain energy back into the power supply.

Problems were especially serious in the electronics for the applique ceramics. The applique ceramics use high voltages (i.e., 0 to 700 Volts) to achieve the required expansion. The task of providing a high voltage power supply that overcame these issues proved to take longer than was available. Eventually an actuator power supply that was open loop in the high power stage had to be accepted. This has severely limited the usefulness of the applique ceramics.

The data shown in Figs. 3 and 5 are from the breadboard electronics using the flight ceramic applique. The high voltage drivers were commercial amplifiers based on vacuum tubes. Each amplifier is larger and weighs more than the entire STRV-1b experiment. Still, the data proves that the flight ceramic appliques were adequate to do the job if the amplifier could have performed better. The analog data from the translators is almost identical to the data shown. The translators do work with the analog controller on the experiment as delivered to the satellite.

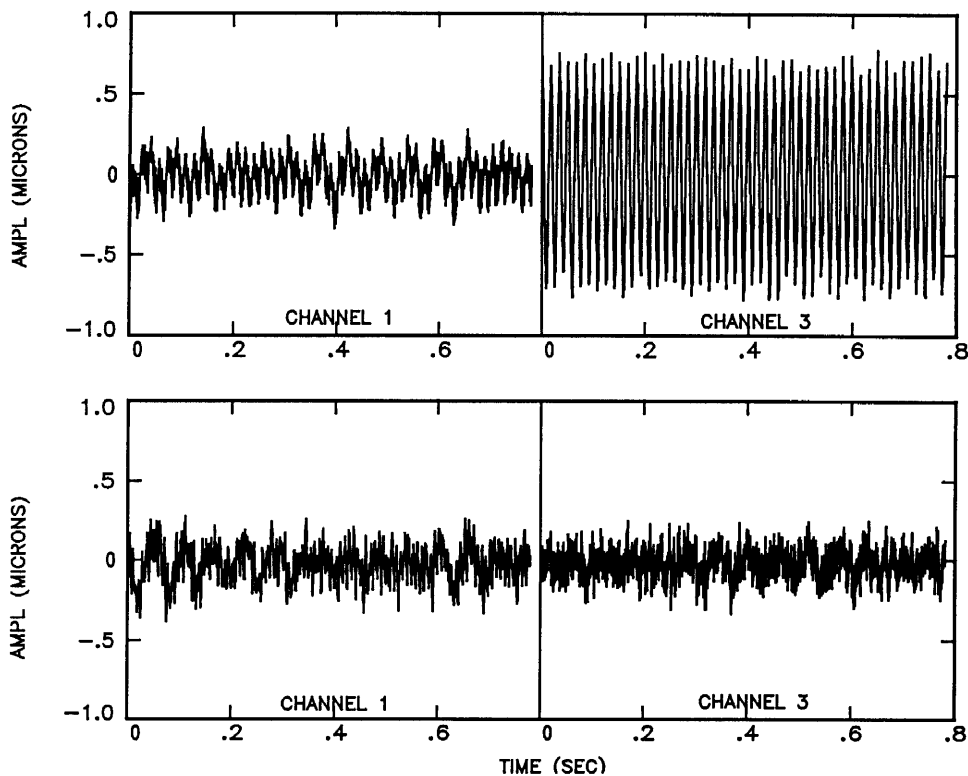


Figure 5. Analog Time Domain Results for Two Channels

DIGITAL CONTROL

The feed-forward control algorithm used in the digital controller is especially well suited to suppressing cryocooler dynamics. This is because the vibration suppression and cooler command are done in the same digital computer. The digital command buffer contains one complete cycle of cooler command multiplexed with three channels of vibration suppression commands. In this configuration the phase angles between the cooler and the vibration suppression are automatically stable even when the frequency changes by changing the sampling rate.

The frequency is changed in an attempt to improve cooler performance by matching the cooler drive frequency to the heat sink temperature. The buffer length is fixed at 80 samples/channel. When the sampling rate changes from 4800 samples/second to 5000 samples/second, the drive frequency changes from 60.0 Hz to 62.5 Hz.

Using uploaded bit-flags, it is possible to configure several algorithms from the code on the satellite. The most promising algorithm starts by commanding pure tones at each actuator for each harmonic frequency. After approximately 15 cycles the system comes to steady state, the response is measured at all three eddy current transducers and averaged in the time domain for 20 cycles, then the next harmonic frequency is tested, etc. This procedure gives the transfer functions used throughout. Since the experiment can only operate for a few minutes due to power limitations, the frequency variation once the experiment is turned on is not significant. If the cooler could be run longer the transfer functions would also be stored at each sampling rate (i.e., cooler drive frequency).

The experiment proceeds by slowly turning on the cooler over a period of several seconds. Then the vibration suppression is turned on. The eddy current time histories are measured and averaged in the time domain over approximately 20 cycles. This average time history is curve

fit using a harmonic expansion to obtain Fourier coefficients at the harmonic frequencies. The integral formulation of this curve fit is illustrated in Eq. (1). The integrals are calculated numerically using Simpson's rule.

$$\begin{aligned}
 \text{signal}(t) &\approx \sum_{i=1}^8 A_i \cos\left(\frac{i 2\pi t}{\text{period}}\right) + B_i \sin\left(\frac{i 2\pi t}{\text{period}}\right) \\
 A_i &= \frac{2}{\text{period}} \int_0^{\text{period}} \text{signal}(t) \cos\left(\frac{i 2\pi t}{\text{period}}\right) dt \quad i = 1, \dots, 8 \\
 B_i &= \frac{2}{\text{period}} \int_0^{\text{period}} \text{signal}(t) \sin\left(\frac{i 2\pi t}{\text{period}}\right) dt \quad i = 1, \dots, 8
 \end{aligned} \tag{1}$$

The integral formulation from Eq. (1) and the least squares estimator, $[X'X]^{-1}X'Y$, are identical over a single cycle. X is simply a matrix of nominal values for sines and cosines. Since a single cycle is used, when the least squares estimator is expanded out, $[X'X]^{-1}$ is just a diagonal of $2/n$, where n is the number of samples in X . $X'Y$ is identical to the Simpson's rule integration from the integral formulation except that the step is in points instead of time. Even the beginning and ending points on the integration agree, since the function is cyclic; thus it is inappropriate to use the beginning and ending factor of $1/2$ typically used with Simpson's rule.

This same curve fit routine was used to tabulate the results of the transfer function calculations using the pure tones as described earlier. At the beginning of the procedure, one-time curve fit results for single frequencies are used to calculate complex transfer functions. Then these transfer functions are inverted using Cramer's rule to calculate the change in command coefficients, C_k , required to cancel the observed eddy current signals, E_i , as shown in Eq. (2).

$$\left[\frac{\partial E_i}{\partial C_k} \right] \{ \Delta C_k \} = \{ -E_i \} \tag{2}$$

The output command time history is updated in the time domain. Then the buffer is output continuously to cancel the eddy current signals. Approximately 15 cycles are allowed to let the transients settle down. The calculated signals are repeatedly output and the whole process is started over updating these signals. It was a surprise how much the controller had to be slowed down to avoid transients. Attempts to speed up lead to instabilities and significant errors. A procedure that helped the stability was to only correct half way to the calculated command value. The series $1/2, 1/4, 1/8, 1/16 \dots$ approaches 1 very rapidly and the controller is considerably more stable.

The results of the digital controller are more dramatic than the results of the analog controller. Fig. 6 illustrates the reduction in harmonic content achieved as a function of time. The top curves are the wideband RMS values for the three eddy current channels. The bottom curves show the harmonic RMS for the controlled frequencies. These two quantities are defined in Eq. (3). Notice that only the eight terms that are being controlled by the digital controller are included in the harmonic RMS.

$$\begin{aligned}
 \text{WIDEBAND RMS} &= \sqrt{\frac{\sum_{i=1}^{\text{buffer}} (\text{signal}(i) - \text{mean signal}(i))^2}{\text{buffer}}} \\
 \text{HARMONIC RMS} &= \sqrt{\sum_{n=1}^8 A(n)^2 + B(n)^2}
 \end{aligned} \tag{3}$$

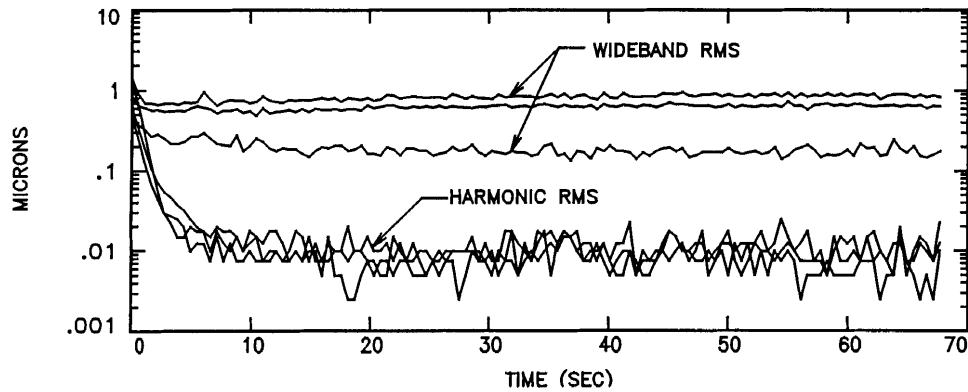


Figure 6. Digital Control RMS and Harmonic Vibration Levels

The wideband results from Fig. 6 are still not fully understood. The wideband RMS should be attenuated much more based on the level of the harmonic attenuation being achieved. A vacuum pump is usually hooked up to the experiment causing vibration and limiting the system performance. Even so, it seems likely that the higher harmonics (8 and 9) are being excited. There are several experiments that can be run once the satellite is in orbit to verify that this is happening. Many other output formats are available from the controller.

Based on the harmonic RMS performance, the results are quite satisfying. Figure 7 illustrates the amount of attenuation achieved. The controller reduces the harmonic amplitude by about 100 times. While more work must be done to be certain, the limitation at a factor of 100 appears to be numerical. There are not enough decimal places in the code to achieve more attenuation. The results are also close to limiting on the 12 bit digitizer or the amount of signal. Finally, the results may be limited by the eddy current sensitivity at 10 nanometers.

The largest challenge encountered was implementing this algorithm on a UTMC 6900 RISC processor with no floating point and no compiler and with the hardware changing up to the last minute. The processor was chosen for speed and radiation hardness. The algorithm had to be programmed in assembly language with implied decimal arithmetic. There was more than adequate speed, and 8K of RAM and 8K of ROM were sufficient. The speed was primarily needed to handle the interrupts associated with the data throughput and still leave time for calculations.

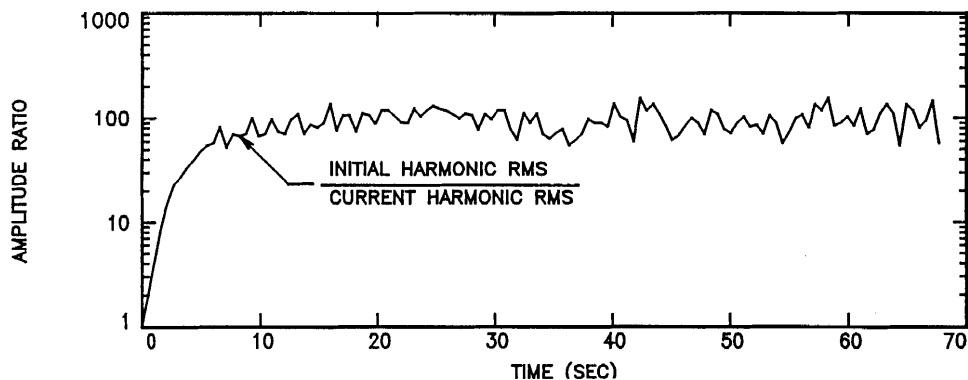


Figure 7. Digital Control Reduction of Harmonic Content

CONCLUSIONS

It is easier to suppress many harmonics of the cryocooler drive signal using a digital controller than an analog controller. The analog controller would have to have three bandpass filters and a 3x3 board for each harmonic frequency. To do any significant number of harmonics using the analog approach would take more circuitry than the digital system. Also physical properties of the plant that may change are built into the analog controller. The transfer functions at the harmonic frequencies have to be solved and inverted for the 3x3 board. While this is easily done while the transfer functions are flat, it is much harder at the higher harmonics. Frequency changes in the cooler can not easily be accommodated in the 3x3 board.

Harmonics beyond the frequencies of the cryocooler supports must be suppressed. This is because the frequency content of the cooler harmonics is so broadband that the support frequencies are sure to be excited. On STRV-1b the supports were made as high frequency as possible. This probably was a mistake. Accepting supports that are just adequate for launch will produce less high frequency content to the cooler harmonics. The part of the harmonics that are amplified by support frequencies would be at a lower frequency. At some frequency above the support frequencies, the supports will isolate the higher harmonics passively.

The commercial translators are easier to use than the ceramic applique. The translators for this kind of vibration suppression do not have to be designed specially. Designing a process such as attaching the applique to the coldfinger is difficult. The translators do not interact directly with the cooler. Gluing applique on the coldfinger made the cooler very difficult to assemble since the coldfinger was out of tolerance in diameter. The ceramic applique changes the cooler performance making steady state unachievable. Most important, the 700 volt requirement for the applique was just too difficult in a severely constrained environment like STRV-1b.

At this writing it is not clear what role there will be for coldfinger motion suppression as opposed force cancellation as proposed in Reference 2. One possibility for an isolated stage would be to mount the cooler on the non-isolated part of the structure and use motion suppression to follow the isolated part of the structure. Force cancellation will not get rid of the small motions suppressed in STRV-1b. These coldfinger motions are driven responses to the pressure variations inside the coldfinger. If motions of this size matter, motion suppression would be the way to suppress them. As the pixel size of sensors gets smaller, motion suppression may actually be required.

The launch is scheduled for June 17, 1994. The remaining questions with respect to the wideband RMS will be answered with flight data.

ACKNOWLEDGEMENT

The work described in this paper was carried out by the Jet Propulsion Laboratory, California Institute of Technology, and was sponsored by the Ballistic Missile Defense Organization/Air Force Phillips Laboratory through an agreement with the National Aeronautics and Space Administration.

REFERENCES

1. Kuo, C. P., "Coldfinger Motion Suppression Using a Ceramic Applique," Proceeding of SPIE's Smart Structures and Materials Conference '93. January 31 - February 4, 1993, Albuquerque.
2. Collins, S. A., Paduano, J. D., von Flotow, A. H., "Multi-axis vibration cancellation for Stirling cryocoolers," Presented at Cryogenic Optical Systems and Instruments VI, April 4-5, Orlando.